Original Article

Senescence Effect on Gastric Parietal Cells in Male Albino Rats and the Impact of Nicotinamide Riboside (a NAD^+ Precursor): Histological Study

Marwa Mohamed Yousry, Abeer Ibraheem Omar and Eman Abas Farag

Department of Histology, Faculty of Medicine, Cairo University, Cairo, Egypt

ABSTRACT

Introduction: Senescence is a normal succession in time and cell maturity with progressive structural and functional cellular changes. Its influence predisposes numerous non-communicable diseases such as neurodegenerative, metabolic and cardiovascular diseases, as well as cancers with subsequent high morbidities and mortalities. Gastrointestinal tract (GIT) manifestations are commonly associated with ageing starting from stomatitis to maldigestion and malabsorption. Nicotinamide adenine dinucleotide [NAD^+], a co-enzyme in oxidative-phosphorylation and redox reactions in metabolism and energy production, is decreased in multiple ageing-associated pathological conditions and its replenishment reveals marked improvement in these conditions.

Aim of the Work: This study aimed at evaluating the senescence sequelae on gastric parietal cells of male albino rats, the probable role of NAD+ and the potential protecting influence of nicotinamide riboside (NR) [a NAD+ precursor].

Materials and Methods: 18 male albino rats were grouped equally into the non-aged group [~3 months, group I], aged group [~24 months, group II] and aged/NR group [~24 months, group III] that received daily single oral dose of 200mg/kg NR for 3 weeks. Just before sacrifice, serum NAD^+, gastrin and pepsinogen-I levels were assessed for all animals. Then, biochemical, histological, immunohistochemical [for H+/K+ ATPase & B-cell lymphoma-2 (Bcl-2)] and morphometric studies were done.

Results: The senescence features demonstrated in the parietal cells of the aged rats were markedly ameliorated with 3 weeks oral intake of NR [a NAD^+ precursor].

Conclusion: Ageing is a systemic process of NAD^+ reduction and consequent oxidative stress, inflammageing, DNA damage and altered apoptosis. Parietal cells ageing results in GIT disturbances that may exacerbate ageing sequelae through induction of anaemia, and continuous NAD^+ reduction. Most manifestations can be blocked by oral supplementation of a NAD^+ precursor, especially NR as it has many advantages over the others.

Received: 24 October 2022, **Accepted:** 19 November 2022

Key Words: Ageing, parietal cell, NAD^+, NAD^+ precursors, nicotinamide riboside.

Corresponding Author: Marwa Mohamed Yousry, MD, Department of Histology, Faculty of Medicine, Cairo University, Cairo, Egypt, **Tel.**: +20 10 0676 3862, **E-mail:** marwa.yousry@cu.edu.eg - marwa.yousry@kasralainy.edu.eg

ISSN: 1110-0559, Vol. 47, No. 1

INTRODUCTION

Ageing is the succession in time and cell maturity as it interacts with the internal and external surroundings. This leads to random and progressive cellular changes in the structure and function[1]. So, ageing is considered a major predisposing factor to numerous non-communicable diseases such as cardiovascular, metabolic, neurodegenerative diseases and cancers. This is, consequently, followed by increased morbidity and mortality rates[2].

Unlike a quiescent cell, a senescent cell will not re-enter the cell cycle in response to any known physiological stimuli. So, stable cell cycle arrest is a defining feature of senescence. Such arrest is known to occur in association with telomere shortening, oncogenic signalling, and extreme DNA damage with deficient repair. These are three hallmarks commonly occurring with ageing[3].

Moreover, senescent cells are characterized by morphological and metabolic changes, chromatin reorganization, and altered gene expression[3]. Furthermore, these cells gain a feature called senescence-associated secretory phenotype [SASP] where they shift their secretory abilities towards secretion of pro-inflammatory cytokines such as interleukin [IL]-1β, IL-6 and tumour necrosis factor [TNF]-α[4].

There is an increased incidence of gastrointestinal tract [GIT] manifestations in elderly including oral ulcers, decreased salivation, decreased secretion of gastric acid, pepsin, and mucus, as well as decreased gastric emptying. Additionally, there is gastric and intestinal malabsorption together with anaemia and anorexia[5].

Nicotinamide adenine dinucleotide [NAD+] is a catalysing co-enzyme in the physiological oxidative phosphorylation and redox reactions in almost all metabolic and energy production processes. These processes include glucose and fatty acid metabolism, cholesterol, and steroid synthesis and Krebs cycle[6].

Bearing in mind that decreased NAD+ is detected in multiple pathological conditions either due to reduction of

 DOI: 10.21608/ejh.2022.170481.1797

its synthesis and/or increased its utilization[7]. Accordingly, increasing NAD+ level is used as an effective therapeutic agent in multiple disorders like cardiovascular diseases [hypertension, heart failure and myocardial infarction], neurodegenerative and cognitive diseases [Alzheimer's and Parkinson's] and metabolic ones [diabetes type II and non-alcoholic fatty liver] which are common ageing diseases[8,9,10].

AIM OF WORK

This study aimed at assessing the effects of ageing on the gastric parietal cells of male albino rats and the possible role of NAD+ in the process, in addition to, the potential protective role of nicotinamide riboside (NR) [one of the NAD+ precursors].

MATERIALS AND METHODS

Experimental Design

Six adult male albino rats (Rattus rattus) aged ~3 months[11] together with another twelve old rats aged ~24 months[11] were used in this study. The rats were housed in Laboratory Animal House Unit of Kasr Al-Aini, Faculty of Medicine, Cairo University, fitting the guidelines stated by Cairo University-Institutional Animal Care and Use Committee (CU-IACUC) [approval number CU/III/F/28/21]. Before starting the experiment, all rats were kept under the same environmental conditions for 48 h to adapt to the new environmental conditions. They were provided with ordinary chow and water ad libitum and housed at 24 ± 1°C in a normal light/dark cycle.

The rats were divided into three main groups:

Group I (non-aged group, 6 adult rats aged 3 months): The rats of this group were considered as control for non-aged rats. They were subdivided equally into: subgroup Ia which received nothing for three weeks, and subgroup Ib which received daily single oral dose of 1 ml distilled water for three weeks. Then, the animals were sacrificed with groups II & III, respectively.

Group II (aged group, 6 old rats aged 24 months): Animals of this group received nothing for three weeks. They were used to evaluate the effect of ageing on the gastric parietal cells.

Group III (aged/NR group, 6 old rats aged 24 months): Each animal of this group received daily oral dose of 200 mg/kg NR dissolved in 1 ml distilled water for three weeks[12] to detect the effect of NAD+ precursor on the ageing process of gastric parietal cells.

Animal studies

Serological Study

Immediately, after the end of the experimental duration, blood samples from the rats of all subgroups were collected from their tail veins to measure serum levels of NAD+, gastrin and pepsinogens as pepsinogen-I at Biochemistry Department, Faculty of Medicine, Cairo University.

Animals sacrifice

At the end of the 3rd week (experimental duration), all rats of all groups were sacrificed after being fed to activate the parietal cells[13]. This was done at the Laboratory Animal House Unit, where the animals were euthanized by intraperitoneal injection of ketamine (90 mg/kg)/xylazine (15 mg/kg)[14]. The abdomens were opened, and the stomachs of all animals were dissected. Three slices (2-2.5 mm each) from the body of the stomach were sliced to prepare gastric homogenates, paraffin blocks and resin blocks.

Gastric Homogenates and ELISA

Gastric homogenates were prepared at the Biochemistry Department, Faculty of Medicine, Cairo University, based on a previously described methodology [15]. This was done by ELISA according to the manufacturer's instructions to measure the following values using the suitable antibodies:

- NAD+ [ab65348, abcam, USA].
- Reactive oxygen species (ROS, oxidizing agent) [MBS166011, MyBioSource, USA].
- Nuclear factor kappa-B (NFκ-B, transcription factor) [MBS268833, MyBioSource, USA].
- Interleukin-6 (IL-6, pro-inflammatory cytokine) [CSB-E04640r, CUSABIO, USA].

Quantitative real-time polymerase chain reaction (qRT-PCR)[15]

At Biochemistry Department, Faculty of Medicine, Cairo University, the total RNA was extracted, and the complementary DNA was synthesized. Then, the Rotor-Gene 6000 series software version 1.7 (Corbett Life Science, USA), the primers were used to detect the relative mRNA expression of P16INK4a (cyclin-dependant kinases inhibitor and cell cycle arrest effector protein), and the result was expressed as a normalized ratio to the internal control (L7a, a ribosomal protein).

The primer PCR sequences used were

- P16INK4a: Forward 5′-TGCAGATAGACTAGCCAGGGGA-3′ Reverse 5′-CTTCCAGCAGTGCCCGCA-3′.
- L7a: Forward 5′-GAGGCCAAAAAGGTGGTCAAT-3′ Reverse 5′-CCTGCCCAATGCCGAAGTTCT-3′.

Histological Study

Paraffin block preparation

The gastric slices for preparation of paraffin blocks for all animals were fixed in 10% formol saline and then kept for 24 h. Afterwards, they were processed to paraffin blocks. Sections of six μm-thick were cut and stained with:

Hematoxylin and Eosin stain (H&E)[16].

Immunohistochemical staining for

- Beta subunit of the Hydrogen/Potassium ATPase (H+/K+ ATPase) [mouse monoclonal antibody, MA3-923, Invitrogen, Thermo Fisher Scientific,

USA]: it is a specific marker for parietal cells' ATPase channels in the intracellular canaliculi and tubulovesicular system.

- B-cell lymphoma-2 (Bcl-2) [rabbit polyclonal antibody, ab196495, abcam, USA]: an anti-apoptotic marker that appears as a cytoplasmic reaction.

Immunostaining was done using avidin-biotin technique[16]. The sections were boiled for 10 min in 10 mM citrate buffer (cat no 005000) pH 6 for antigen retrieval. Then, they were put to cool for 20 min at room temperature. After that, the sections were incubated with the primary antibodies for 1 h. Immunostaining was accomplished using Ultravision One Detection System (cat no TL - 060- HLJ). Counterstaining was performed using Lab Vision Mayer's hematoxylin (cat no TA- 060- MH).

Negative control sections were prepared by the same process after primary antibody exclusion. Citrate buffer, Ultravision One Detection System and Ultravision Mayer's hematoxylin were purchased from Labvision, ThermoFisher Scientific, USA.

Resin block preparation

The stomach slices for resin block preparation were cut into small fragments (0.5-1.0 mm3) that were prefixed in 2.5 % glutaraldehyde for 2 h and postfixed in 1% osmium tetroxide in 0.1 M phosphate buffer at pH 7.4 and 4 °C for 2 h. Then dehydration and resin embedding were done[16].

Semithin (1 μm) and ultrathin (70–90 nm) sections were cut using a Leica ultra-cut (UCT) (Glienicker, Berlin, Germany). The semithin sections were examined by the light microscope after being stained with toluidine blue (1%) while, the ultrathin sections were stained with uranyl acetate followed by lead citrate then examined by transmission electron microscope (TEM) [JEOL JEM-1400, Japan][16].

Morphometric study

In ten non-overlapping fields (×100) for each group, the area percent of the positive immuno-expression for H+/K+ ATPase and BCL-2 were measured in the corresponding immunostained sections.

Image analysis was done by Leica Qwin-500 LTD-software image analysis computer system (Cambridge, England).

Statistical analysis

The biochemical and morphometric measurements were expressed as mean ± standard deviation (SD). Statistically, they were analyzed using one-way analysis of variance (ANOVA) followed by "Tukey" post hoc test. This was performed using IBM Statistical Package for the Social Sciences (SPSS) version 21. The results were considered statistically significant when *P value* was < 0.05.

All the histological and morphometric studies and the statistical analysis were done at Histology Department, Faculty of Medicine, Cairo University. However, examination of the ultrathin sections was achieved at Electron Microscope Research Unit, Faculty of Agriculture, Cairo University.

RESULTS

General observations

No deaths nor abnormal behaviour were observed in any of the experimental animals.

The two non-aged subgroups showed nearly the same serological, biochemical, and histological results. So, they were collectively named the non-aged group (group I).

Animal Data

Serological Results (Figure 1a)

Serum NAD+ and pepsinogen-I levels showed significant decrease in group II versus group I and group III. In addition, NAD+ level in group III showed a significant decrease while pepsinogen-I level revealed a non-significant decrease compared to group I. Conversely, the serum level of gastrin revealed a significant increase in the aged group compared to both non-aged and aged/NR groups and a non-significant increase in aged/NR group versus non-aged group.

ELISA Results for NAD+, ROS, NFκ-B, IL-6 and qRT-PCR results for P16INK4a (Figures 1b – 1d)

Group II revealed a significant decrease in NAD+ level and significant increase in the levels of ROS, NFκ-B, IL-6, and P16INK4a when compared with groups I & III. On the other hand, group III demonstrated a significant decrease in NAD+ level, a significant increase in P16INK4a and a non-significant increase in the ROS, NFκ-B, and IL-6 levels versus group I.

Histological Results

Group I (non-aged group): H&E-stained sections of the oxyntic mucosa (Figure 2a) revealed that it was formed of gastric pits and oxyntic glands. The pits were visualized as surface epithelial invagination conducting the glands' secretions to the surface where each pit received 2 or more oxyntic glands. The pits were lined with foveolar cells (surface mucous-secreting cells). However, the oxyntic glands were highly crowded with minimal CT corium in-between. They occupied 3⁄4 of the mucosa and organised perpendicular to its surface with a pit: gland volume ratio, 1:3. Each gland was arranged into isthmus, neck, and base.

Parietal and chief cells were the main cellular components of the glands. Since the parietal cells were visualized as the main cells in the upper half of the gland where they were accompanied by mucous neck cells. While in the lower half of the gland, the chief cells were the principal cells together with some parietal cells.

The mucous-secreting foveolar and mucous neck cells appeared with apically vacuolated and totally vacuolated cytoplasm, respectively. The chief cells were seen with basophilic cytoplasm; however, the parietal cells were large, triangular to rounded with deeply acidophilic cytoplasm and central rounded nuclei.

Toluidine blue-stained sections of the oxyntic glands' lower halves (Figure 2b) showed chief and parietal cells. The chief cells were seen as cuboidal cells with dense cytoplasm, rounded basal vesicular nuclei, and apical zymogen granules. However, the parietal cells were large rounded or pyramidal having narrow apices bulging into the lumen. They had central large, rounded nuclei with almost uniformly distributed chromatin. Their cytoplasm appeared dense with numerous spherical cytoplasmic densities.

H+/K+ ATPase immunostained sections demonstrated abundant positive cytoplasmic and membranous immunostaining in the parietal cells (Figure 2c).

Bcl-2 immunostained sections showed that the positive immunoreaction was scarcely spread throughout the cytoplasm of the oxyntic mucosal cells, including the parietal cells (Figure 2d).

The ultra-thin sections of this group (Figures 2e-2i) paraded normal ultra-structure of the parietal cells. They were cells with central rounded large pale nuclei and narrow apices towards the lumina. Their apical cell membranes were provided with microvilli that demonstrated dense cortex and less dense core. The cells rested on a continuous basement membrane, where the basal cell membrane showed slight infolding, not including the basement membrane. The cells' lateral membranes in contact with the other parietal cells or with the chief cells were almost straight.

The parietal cells' cytoplasm revealed numerous intracellular canaliculi loaded with multiple long interdigitating microvilli that demonstrated dense cortex just beneath the membrane and less dense core with slightly dense dots or fibrils in-between. In addition, there was a tubule-vesicular system very close to these canaliculi and consisted of vesicles (either small irregular or large rounded) and tubules that barely connecting the vesicles.

In addition, the cytoplasm exhibited numerous large dense mitochondria that seemed to be in two groups; the first one was close to the cell membrane while the second one appeared around the nucleus. Sometimes, these two groups are separated by a pale cytoplasmic area with crowded irregular vacuoles. Moreover, there were multiple inclusion microbodies (most probably glycogen) that were smaller than mitochondria and of heterogenous densities.

Some of the sections at the base of the oxyntic glands showed chief cells in addition to the parietal cells. The chief cells exhibited features of protein synthesizing cells: euchromatic nuclei, mitochondria, widely spread rER, and zymogen granules.

Group II (aged group): H&E-stained sections (Figure 3a) appeared similar to that of the non-aged group with slight disorganization of the oxyntic glands.

The semi-thin sections (Figure 3b) established features of senescence in the parietal cells. The cells were enlarged with almost flattened luminal surface. They exhibited irregular nuclei with multiple dense foci. Their cytoplasm showed few spherical cytoplasmic densities, and numerous rounded pale stained vacuoles that sometimes appeared fused. Additionally, chief cells showed irregularity of their nuclei and reduced zymogen granules.

H+/K+ ATPase immunostained sections verified marked reduction in the positive immunoreaction in the parietal cells (Figure 3c).

Bcl-2 immunostained sections confirmed widely distributed immunopositivity in most of the mucosal cells, including the parietal cells (Figure 3d).

Ultra-structurally (Figures 3e-3i), the senescent parietal cells revealed almost flat apical membranes, as their microvilli became few, short, and wide. Their nuclei seemed irregular with disrupted membranes and heterochromatic foci. Moreover, the cytoplasm demonstrated few intracellular canaliculi with few, short, & dilated microvilli and multiple vesicles that sometimes seemed fused and dilated. Some tubules appeared fused with vesicles, and others were dilated. Few glycogen microbodies, and numerous degenerated mitochondria were seen. In addition, there were few basal infoldings of the basal cell membrane with degenerated mitochondria. In addition, peptic cells appeared with heterochromatic foci of their nuclei and degenerated mitochondria.

Group III (aged/NR group): H&E-stained sections (Figure 4a) revealed almost normal appearance of the oxyntic mucosa with regularly arranged oxyntic glands.

In the semi-thin sections (Figure 4b), the parietal cells appeared very close to those in the non-aged group. However, few cells were enlarged and presented with irregular nuclei. Few of these nuclei demonstrated dense foci. Moreover, most of the chief cells showed regular nuclei and numerous zymogen granules, similar to those of the non-aged group.

In H+/K+ ATPase immunostained sections (Figure 4c), the positive immunoreaction was abundantly spread in the parietal cells.

Bcl-2 immunostained sections (Figure 4d) proved dispersed positive immunoreaction in the mucosal cells of the oxyntic glands, including parietal cells.

In the ultra-thin sections (Figures 4e-4g), the parietal cells nearly displayed the same ultrastructure as those in the non-aged group, but few cells showed irregular nuclei with heterochromatic foci and few dilated tubules. The chief cell appeared almost like that of the non-aged group.

Morphometric Results

Statistically, the mean area percent of H+/K+ ATPase positive immunoreaction of the parietal cells indicated a significant decrease in the aged group versus non-aged and aged/NR groups. In addition, it showed a non-significant decrease in the aged/NR group compared to the non-aged group (Figure 5a). This came in contrast to the statistical analysis of the mean area percent of Bcl-2 positive immunoreaction which revealed a significant increase in group II versus groups I and III in addition to its significant increase in group III in comparison with group I (Figure 5b).

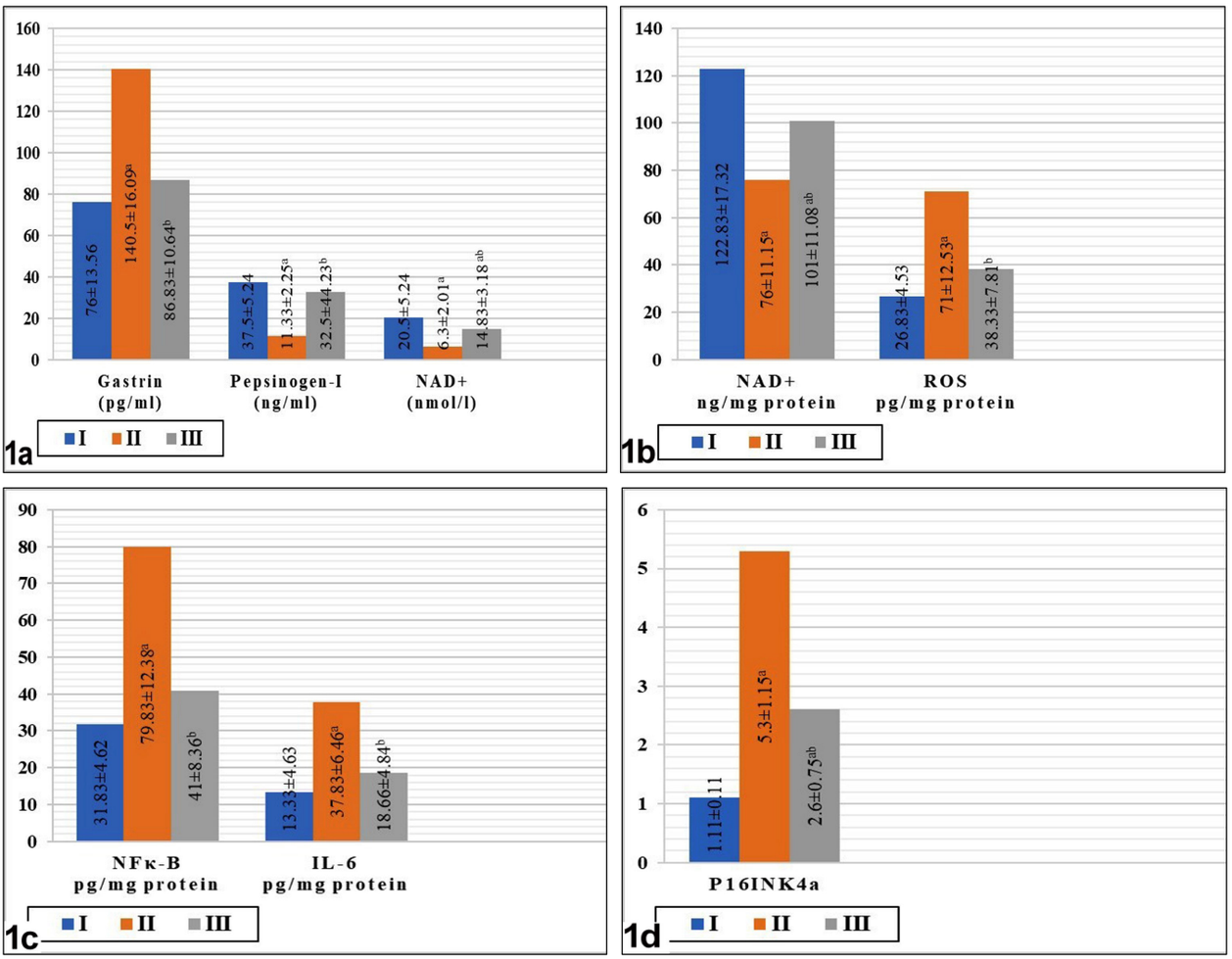

Fig. 1: Showing mean values of: 1a: Serum gastrin, pepsinogen-I & NAD+ levels. 1b: Stomach homogenate NAD+ and ROS levels. 1c: Stomach homogenate NFκ-B, IL-6 levels. 1d: P16INK4a relative mRNA expression. [a as compared to group I & b as compared to group II (significant difference at $P < 0.05$)]

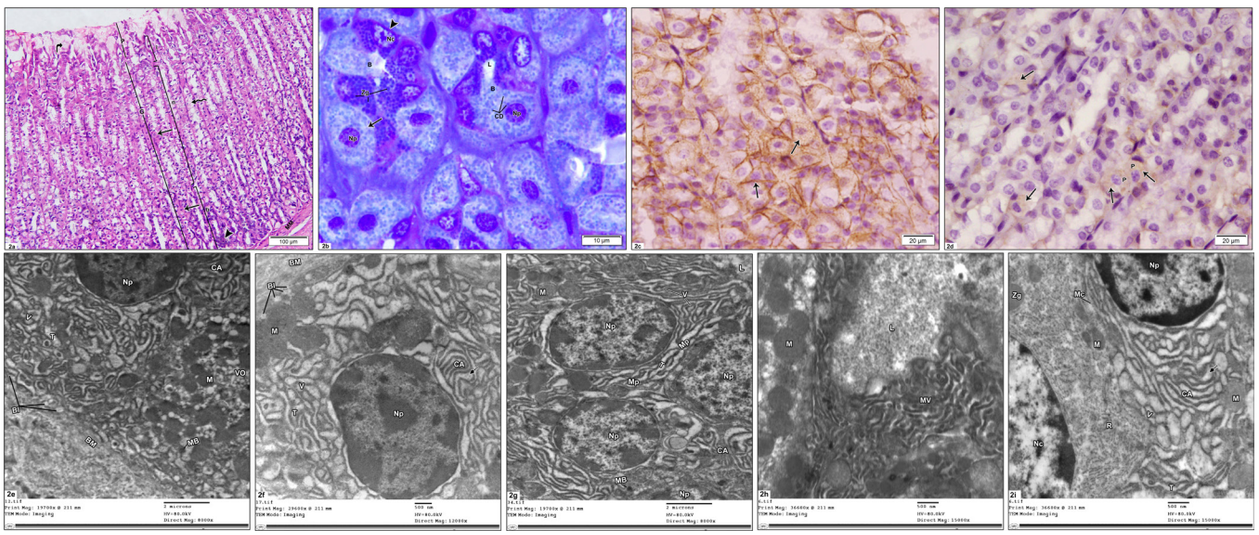

Fig. 2: Photomicrographs of sections in the stomach body of the non-aged group (group I).

2a: Oxyntic mucosa shows gastric pits (P) and oxyntic glands (G) in a ratio of 1:3, as well as muscularis mucosa (MM). The glands are highly crowded with minimal CT corium in-between, and they are divided into isthmus (i), neck (n), and base (b). Foveolar cells with apical cytoplasmic vacuolations (right-angled arrow), line the pits. The upper halves of the glands are lined mainly by parietal cells that appear as large, triangular to rounded cells with deeply acidophilic cytoplasm and central rounded nuclei (arrow) and mucous neck cells with completely vacuolated cytoplasm (wavy arrow). The lower halves of the glands reveal mainly chief cells with basophilic cytoplasm (arrowhead), and some parietal cells (arrow). [H&E, x100]

2b: The lower halves of the oxyntic glands demonstrate chief (arrowhead) and parietal cells (arrow). The chief cells are cuboidal cells with dense cytoplasm, rounded basal vesicular nuclei (Nc), and apical zymogen granules (Zg). The parietal cells are large rounded or pyramidal cells having central large, rounded nuclei (Np) with uniformly distributed chromatin, dense cytoplasm with numerous spherical deeply stained vacuoles (CD), and narrow apices bulging (B) into the lumen (L). [Toluidine blue, x1000]

2c: Abundant positive membranous and cytoplasmic immunostaining (arrows) in the parietal cells. [anti H+/K+ ATPase immunohistochemical stain, x400]

2d: Scarcely spread positive cytoplasmic immunoreaction (arrows) throughout the oxyntic mucosal cells cytoplasm including the parietal cells (P). [anti Bcl-2 immunohistochemical stain, x400]

2e: A part of parietal cell base is seen resting on continuous basement membrane (BM) with numerous basal membrane infoldings (BI), rounded euchromatic nucleus (Np), numerous microbodies (MB), multiple intracellular canaliculi (CA) with multiple long interdigitating microvilli, some tubules (T) and vesicles (V). Multiple mitochondria (M) are seen distributed near the nucleus and near the cell membrane and separated by a pale cytoplasmic area with numerous irregular vacuoles (VO). [TEM, x8000]

2f: Higher magnification of a part of parietal cell base resting on basement membrane (BM) reveals multiple basal infoldings (BI) with multiple basal mitochondria (M), euchromatic nucleus (Np), intracellular canaliculi (CA) with multiple long interdigitating microvilli that illustrate dense cortex just beneath the membrane and less dense core with slightly dense dots or fibrils in-between (dashed arrow), vesicles (V) and tubules (T) that barely connect with the vesicles. [TEM, x12000]

2g: Parts of four parietal cells are visualized with almost straight lateral membranes in-between them (Mp), narrow apices towards the lumen (L) and central large rounded pale nuclei (Np). Their cytoplasm reveals intracellular canaliculi (CA), tubules (T) and vesicles (V), numerous large dense mitochondria (M) either close to the cell membrane or around the nucleus and multiple small inclusion microbodies (MB) with heterogeneous densities. [TEM, x8000]

2h: Higher magnification of apical parts of parietal cells reveals their apical membranes numerous long interdigitating microvilli (MV) with dense cortex and less dense core projecting into the lumen (L) and multiple mitochondria (M). [TEM, x15000]

2i: A Part of parietal cell shows rounded euchromatic nucleus (Np), mitochondria (M), intracellular canaliculi (CA) with long interdigitating microvilli demonstrating dense cortex and less dense core with slightly dense dots or fibrils in-between (dashed arrow), irregular small or large rounded vesicles (V), tubules (T) and almost straight lateral cell membrane (Mc) with the chief cell. A part of chief cell is also noticed with euchromatic nucleus (Nc), mitochondria (M), widely spread rER (R), and zymogen granules (Zg). [TEM, x15000]

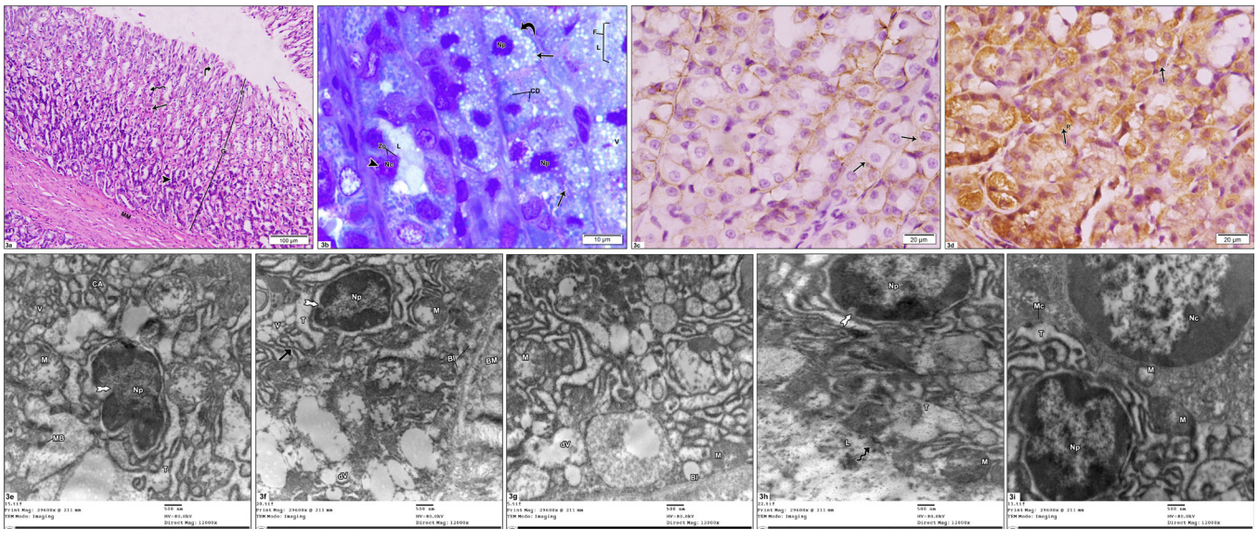

Fig. 3: Photomicrographs of sections of stomach body of the aged group (group II).

3a: Oxyntic mucosa of slightly disorganized gastric glands (G) is seen limited by muscularis mucosa (MM). The glands open into gastric pits (P) with foveolar cells lining (right-angled arrow). Parietal cells (arrow), mucous neck cells (wavy arrow) and chief cells (arrowhead) are noticed lining the oxyntic glands. [H&E, x100]

3b: Senescent parietal cells (arrows) are noted as enlarged cells with almost flattened apical surface (F) into the lumen (L) and irregular nuclei (Np) with multiple dense foci. Their cytoplasm shows few spherical cytoplasmic densities (CD) and numerous rounded pale stained vacuoles (V) that sometimes appear fused (curved arrow). Chief cells (arrowhead) reveal irregular nuclei (Nc) and reduced zymogen granules (Zg). [Toluidine blue, x1000]

3c: Markedly reduced positive membranous and cytoplasmic immunoreaction (arrows) in the parietal cells. [anti H+/K+ ATPase immunohistochemical stain, x400]

3d: Widely distributed cytoplasmic immunopositivity (arrows) throughout most of oxyntic mucosal cells including the parietal cells (P). [anti Bcl-2 immunohistochemical stain, x400]

3e: A senescent parietal cell reveals irregular nucleus (Np) with heterochromatic foci and disrupted nuclear membrane (bifid arrow), cytoplasmic intracellular canaliculi (CA) with few, dilated short microvilli, multiple vesicles (V), and dilated tubules (T), few microbodies (MB), and multiple degenerated mitochondria (M). [TEM, x12000]

3f: Basal part of an aged parietal cell appears with an irregular nucleus, foci of heterochromatin (Np) and disrupted nuclear membrane (bifid arrow). Its basal cell membrane rests on a straight basement membrane (BM) and shows few basal infoldings (BI). The cytoplasm reveals multiple degenerated mitochondria (M) with disrupted cristae, multiple vesicles (V) that sometimes appeared fused and dilated (dV) in addition to dilated tubules (T). Some of these tubules fuse with the vesicles (arrow). [TEM, x12000]

3g: Higher magnification of a part of parietal cell base demonstrates few basal infoldings (BI), dilated tubules (T), dilated vesicles (dV) and degenerated mitochondria (M) with disrupted cristae. [TEM, x12000]

3h: A part of parietal cell apex with almost flat apical cell membrane (wavy arrow) is detected in the lumen (L). Its nucleus with foci of heterochromatin (Np) and disrupted nuclear membrane (bifid arrow) is also seen. Degenerated mitochondria (M) and dilated tubules (T) are visualized. [TEM, x12000]

3i: A part of chief cell is seen with nuclear heterochromatic foci (Nc), degenerated mitochondria (M) and nearly straight lateral cell membrane (Mc) with a parietal cell. The parietal cell exhibits irregular nucleus with foci of heterochromatin (Np), degenerated mitochondria (M) and dilated tubules (T). [TEM, x12000]

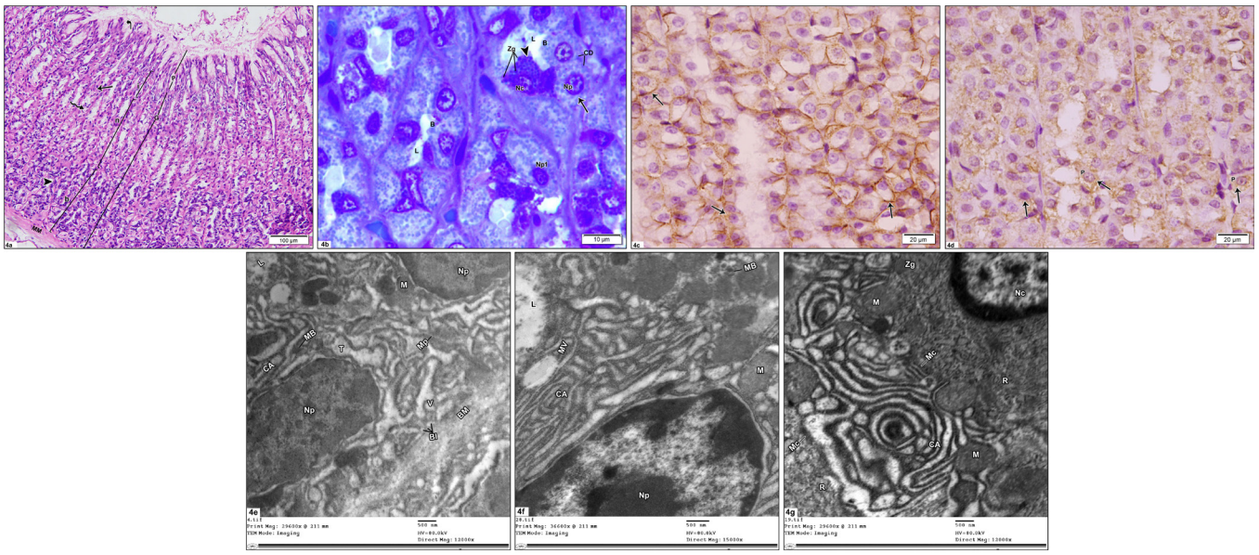

Fig. 4: Photomicrographs of sections in the body of the stomach of the aged/NR group (group III).
4a: Oxyntic mucosa of regularly arranged crowded oxyntic glands (G) divided into isthmus (i), neck (n) & base (b), gastric pits (P), and muscularis mucosa (MM) is detected. The pits are lined with foveolar cells (right-angled arrow), while the oxyntic glands are lined by parietal cells (arrow), mucous neck cells (wavy arrow), and chief cells (arrowhead). [H&E, x100]
4b: Most of the parietal cells (arrow) appear with narrow apices bulging (B) into the lumen (L), central rounded pale nuclei (Np) and spherical cytoplasmic densities (CD). Few parietal cells appear with irregular nuclei (Np1) and dense foci. Most of the chief cells (arrowhead) demonstrate almost regular nuclei (Nc) and numerous zymogen granules (Zg). [Toluidine blue, x1000]
4c: Abundant spread of positive membranous and cytoplasmic immunoreaction (arrows) in the parietal cells. [anti H+/K+ ATPase immunohistochemical stain, x400]
4d: Dispersed positive cytoplasmic immunostaining (arrows) throughout the mucosal cells including the parietal cells (P). [anti Bcl-2 immunohistochemical stain, x400]
4e: Parts of two parietal cells contact each other by almost straight lateral cell membranes (Mp), rest on straight basement membrane (BM) by their basal cell membranes that show multiple basal infoldings (BI). Their cytoplasm shows mitochondria (M), microbodies (MB), intracellular canaliculi (CA), few vesicles (V) and few dilated tubules (T). Their nuclei are irregular with foci of heterochromatin (Np). Notice the appearance of the lumen (L). [TEM, x12000]
4f: A part of parietal cell apex shows an euchromatic nucleus (Np), multiple mitochondria (M), microbodies (MB), long interdigitating microvilli forming intracellular canaliculi (CA) and apical microvilli (MV) within the lumen (L). [TEM, x15000]
4g: A part of parietal cell with chief cells on either side are seen. The chief cells demonstrate euchromatic nucleus (Nc), numerous rER (R), mitochondria (M), zymogen granules (Zg) and nearly straight lateral cell membranes with a parietal cell (Mc). Intracellular canaliculi (CA) and mitochondria (M) are seen within the cytoplasm of the parietal cell. [TEM, x12000]

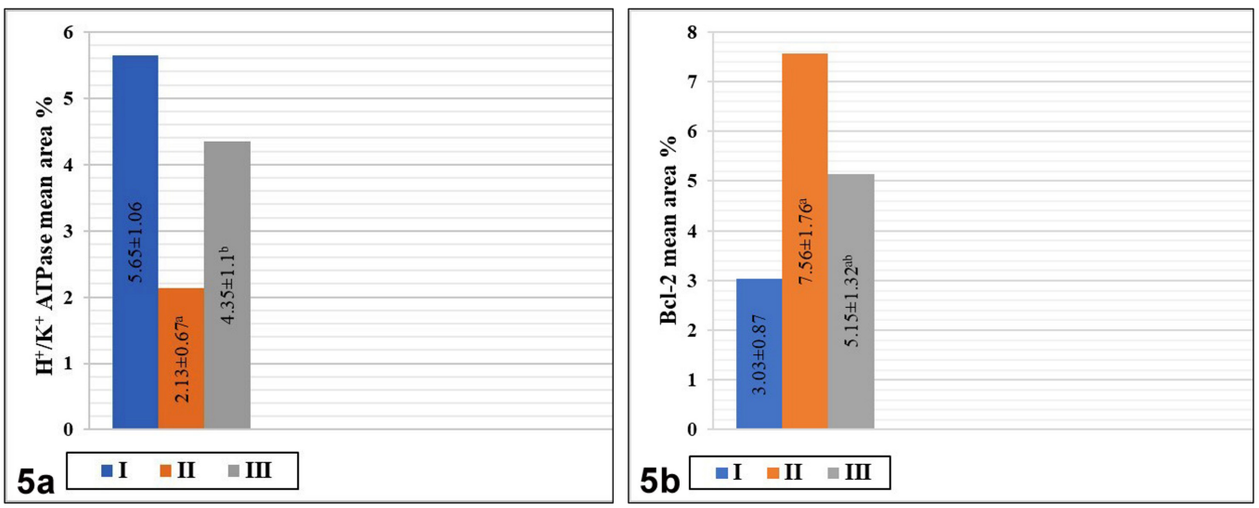

Fig. 5:
5a: Demonstrating the mean area % of H+/K+ ATPase positive cells. [a & b as compared to group I & group II, respectively (Significant difference at $P < 0.05$)]
5b: Demonstrating the mean area % of Bcl-2 positive cells. [a & b as compared to group I & group II, respectively (Significant difference at $P < 0.05$)]

DISCUSSION

This study targeted at evaluating the consequences of ageing on the gastric parietal cells of male albino rats with highlighting the possible role of NAD+. In addition, it assessed the probable protective value of nicotinamide riboside (NR) [one of the NAD+ precursors].

The gastric parietal cells were used in this study as they are considered one of the main controllers of the GIT functions. This occurs through their secretion of hydrochloric acid [HCl], the main activator for digestion of food, absorption of iron, calcium, and vitamin B12, in addition to its role in bacterial growth control. Moreover, HCl was reported to regulate the production of hormones like gastric gastrin, and ghrelin as well as intestinal motilin secreted by the neuroendocrine cells [G-, X-, and Mo-cells, respectively][17] along with gastric leptin[18]. Also, parietal cells were stated to secrete multiple growth factors like transforming growth factor [TGF]- α and epidermal growth factor [EGF] that mediate the GIT mucosal cell proliferation[17].

Cellular senescence that appeared in the gastric parietal cells of the aged rats (group II) was considered as a part of the whole-body ageing process[1]. Such process could be explained by oxidative stress [OS][19] which in turn could be enlightened based on the previously reported decline in the systemic level of NAD+ during the ageing process[20].

NAD+ is the main co-factor for the majority of dehydrogenases of most oxidation/reduction and energy supply reactions in the body through its reversible transformation into NADH[6,21]. Thus reduced NAD+ level is followed by alteration of these reactions, mitochondrial dysfunction, and consequently accumulation of ROS. Such explanation was supported in this study by the significant decrease in the serum level of NAD+ and the subsequent significant decrease in its gastric homogenate level in group II when compared to group I. Moreover, there was a significant increase in the stomach homogenate level of ROS in the aged group versus the non-aged one.

Decreased NAD+ was also stated to be responsible for the ageing-associated genomic instability and DNA damage (an important ageing hallmark)[3,22]. This might occur through induction of OS and high levels of ROS[22] or via decrease in the activity of sirtuin deacetylases, the NAD+-dependant enzyme responsible for DNA repair[7]. Such instability was stated to affect both nuclear and mitochondrial DNA[3].

The ageing-induced altered mitochondrial DNA is coupled with mitochondrial dysfunction that is manifested by defective oxidative phosphorylation, Krebs cycle, and β-oxidation[23]. Consequently, there is production of lots of mitochondrial ROS and more OS[18,22]. This adds to the explanation of the significant increase in the ROS level, and the presence of multiple degenerated mitochondria in the parietal cells of the aged group versus the non-aged group.

However, the disturbed nuclear DNA associated with ageing was described to result in disruption, mutation and/or inactivation of genes[3]. Disruption of the genes responsible for lamins production leads to their defective functions and the consequential disruption of the nuclear lamina [a common feature of ageing-induced nuclear DNA alteration][24]. This was backed in the aged group of this work by the presence of irregular nuclei of parietal cells with disrupted nuclear membrane in addition to the appearance of multiple heterochromatic foci representing the inactive genes.

Moreover, this study's aged group demonstrated senescent cells SASP where there was a significant increase in the gastric homogenate level of IL-6 (a pro-inflammatory cytokine) when compared to its level in the non-aged group. This finding could be explained by the significant increase in NFκ-B (transcription factor for pro-inflammatory cytokines) homogenate level in this group versus the non-aged group. Such explanation was reinforced by the similarly reported significant NFκ-B increase in a previous study[25] following senescence induction in melanoma cells. In addition to the further enforcement achieved from a former study which stated that the responsibility of NFκ-B for the inflammageing process through induction of production of pro-inflammatory cytokines, such as IL-1β, IL-6, and TNF-α, from the senescent cells[25].

Ageing-associated increase in NFκ-B could be illuminated by NAD+ decline accompanying the senescence process through two mechanisms: First, marked elevation of ROS during ageing[26]. Second, the reduction in sirtuin deacetylases like SIRT1, 2 & 6 [NAD+-dependant enzymes responsible for protein deacetylation, proper mitochondrial functions, effective stem cells, DNA repair and efficient metabolic pathways[27,28] secondary to NAD+ decline[3].

The relationship between the senescent cells and apoptosis is characterized by being contradictory where ageing could induce apoptosis in certain cells and prevent it in other cells[29]. This conflicting reaction could be explained by the chronic genomic stress and persistent DNA damage response (DDR) induced by NAD+ reduction during the process of ageing[7]. This DDR could be followed by either over-activation or mutation of certain genes like P53 gene (the tumour suppressor gene)[30].

Activation of P53 gene with consequent increased P53 protein might result in apoptosis. This was documented in the non-regenerative cells like nerve cells and cardiac muscle cells with the consequent neurodegenerative and cognitive diseases, as well as cardiovascular diseases commonly associated with ageing[29]. In other cells like rapidly dividing cells, increased P53 protein is ensued by the arrest of the cell cycle from G1 phase to S phase. Such arrest was documented to occur via expression of P16 gene and production of P16INK4a protein that inhibits the cyclin-dependent kinases (CDKs) responsible for the progression of the cell cycle[31,32].

However, in rapidly regenerating cells like GIT mucosal cells, P53 gene is mutated[33]. The mutated P53 protein activates Bcl-2 and other anti-apoptotic molecules and suppresses the pro-apoptotic molecules like Bax resulting in repression of apoptosis of these cells[22]. Therefore, regeneration of these cells from the stem cells stops, as their apoptosis is the main stimulus for their regeneration[29]. All these paradoxical apoptotic reactions of the ageing cells were assumed to prevent tumour production from the ineffective senescent cells with damaged DNA (a protective measure of senescence)[3,32].

Accordingly, the gastric mucosal cells in the aged group of this study revealed significant increase in the homogenate level of P16INK4a protein and in the mean area percent of Bcl-2 immunoreaction compared to the non-aged group. This was presumed to be due to the ageing of the undifferentiated stem cells (rapidly dividing cells) and the rapidly regenerating cells, correspondingly.

The senescent parietal cells in group II established morphological features of decreased HCL secretion (resting cell phase) although the animals were sacrificed after being fed. These findings are consistent with that previously discovered in the parietal cells of starved rats[34]. The cells showed decreased intracellular canaliculi with few short and dilated microvilli, multiple intracellular vesicles, and tubules where some of them appeared fused. In addition, their apical cell membranes revealed slight plication with few short wide microvilli. These findings were backed by the significant decrease in H+/K+ ATPase [the pump responsible for forcing H+ in the gastric lumen in exchange with K+ to form HCL[17], in group II in comparison with group I.

The decreased HCL secretion even after food stimulation could be elucidated by the reduction of NAD+ accompanying the ageing process. This reduction leads to ineffective oxidation/reduction reactions and defective ATP production which is considered a motor for H+/K+ ATPase pump[17]. Moreover, chronic gastritis, a part of the inflammageing state induced by the pro-inflammatory cytokines production (SASP), was reviewed to affect the parietal cells and decreased their HCL secretion[17].

Another explanation for the reduced HCL secretion was achieved through lowered parietal cells' response to gastrin hormone[33] despite its increased secretion detected in the aged group of the current study in comparison to the non-aged group. Increased gastrin secretion was reported to occur secondary to low level of HCL[35]. The parietal cells diminished response could be enlightened by the decrease in their gastrin receptors documented previously in cases of ageing[33].

Decreased level of HCL has multiple sequelae, for example, decreased serum level of pepsinogen-I (one of the pepsinogens secreted by the oxyntic chief cells) which was confirmed in the aged group of this study versus the non-aged group, in addition to the decreased chief cells' zymogen granules detected in this work. In the stomach, such pepsinogens get activated into pepsin by the gastric HCL. High serum gastrin and low serum pepsinogen-I were assumed to be good indicators for reduced HCL secretion based on a previous study where these findings were reported with hypochlorhydria induced by chronic atrophic gastritis[36]. Decreased HCL, pepsinogen-I, and pepsin lead to maldigestion and concomitant malabsorption of nutrients[37].

Additionally, reduced HCL decreases the intestinal motilin secretion which, in turn, delays gastric emptying as motilin is secreted during fed stage by high H+ to act in the fasting stage[38]. Diminished HCL is followed by increased secretion of gastric leptin (anti-feeding hormone) and consequently decreased secretion of ghrelin (feeding hormone) [leptin/ghrelin cross talk][39,40]. All these sequalae were documented to result in maldigestion, malabsorption, anorexia, and decreased food intake commonly associated with age[5].

Moreover, ageing reduced HCL is frequently associated with gastric malabsorption of iron, calcium, and vitamin B12 with subsequent different types of anaemia (microcytic or pernicious anaemia), decreased energy production and different neurological manifestations[5,18]. Furthermore, absence of the proper control of gastric bacteria via reduced HCL secretion flares up the bacterial growth (e.g., Helicobacter Pylori)[41] that might add to the state of ageing chronic gastritis and may lately result into atrophic gastritis with more and more GIT manifestation.

So, all these GIT senescence manifestations induced by the senescent parietal cells were clarified to be due to ageing-associated decrease in NAD+ level. This reduction was reported to be due to either decrease in its biosynthesis or increase in its utilization[21,42].

Increased NAD+ utilization was documented during ageing process. It occurs due to over activation of NAD+-dependent enzymes such as poly-ADP-ribose polymerases [PARPs], especially PARP1, and sirtuin deacetylases, trying to correct the ageing-associated increase in DNA damage, and impaired metabolism[42]. In addition, increased level of CD38 [NADase enzyme that hydrolyses NAD+] was proved during ageing due to ageing-induced high level of active NFκ-B and subsequent chronic inflammation[43,44]. Such increase in these enzymes' activity, especially PARP1 and CD38 with subsequent depletion of NAD+ was documented to decrease these enzymes' activity, especially that of sirtuin deacetylases and so on, creating a vicious circle between reduced NAD+ and reduced enzymatic activity[42].

Regarding NAD+ synthesis, it occurs through two main ways: de novo synthesis from tryptophan and salvage pathway of its precursors [nicotinic acid (NA), nicotinamide (NAM), nicotinamide mononucleotide (NMN), and nicotinamide riboside (NR)]. The main precursor in mammals is NAM which is then converted into NMN by nicotinamide phosphoribosyl transferase (NAMPT, the key enzyme). Then, NMN is converted into

NAD+. NMN can also be synthesized directly from NR by NR-kinases (NRKs)[7,45].

Ageing-associated defect in the NAD+ de novo synthesis could be explained by the fact that this type of synthesis is a long multistep process that needs a lot of energy[7]. Besides, it depends on the ingestion and absorption of tryptophan which is provided in minimal amount in diet and not converted into NAD+ in all tissues[27]. During ageing, there were defective energy supply, anorexia and malabsorption induced by parietal cells senescence.

Whereas NAD+ synthesis by salvage of its precursors was documented to be insufficient during ageing due to marked increase in NAD+ utilization over its salvage synthesis pathway capacity, in addition to the ageing-induced reduction in NAMPT enzyme[7]. Moreover, the very low amount of these precursors in diet which is subjected to senescent parietal cells-induced defective intake and malabsorption[27].

Accordingly, the proper way to control all these ageing manifestations is to increase NAD+ level[45]. It was presumed that the most effective way to elevate NAD+ level is via supplementation of its precursors to increase the rate of its production through their salvage[7,45]. This suggestion was proved in the aged/NR group of this study where NAD+ serum and gastric homogenate levels showed significant increase from those of the aged group despite their significant decrease than those of the non-aged group. Moreover, the gastric homogenate level of P16INK4a and the mean area percent of Bcl-2 positive immunoreaction revealed significant decrease versus group II although they showed significant increase versus group I. Otherwise, all other morphological, biochemical, and statistical results reported in the aged/NR group showed non-significant differences from those in the non-aged group.

Nicotinamide riboside (NR), one of these precursors, was chosen in this study due to its advantages over the other precursors[7]. It has the best oral bioavailability among all NAD+ precursors[46]. Additionally, it can be converted directly into NMN by a NR-kinases (NRKs) providing a shorter way to synthesis NAD+ bypassing the need for NAMPT which was documented to decrease by ageing[7,45]. Moreover, NR is a safe, well-tolerated precursor without any side effects such as painful flushing sensation and pruritis reported with NA and NAM[47]. Besides, NAM fails to increase sirtuin deacetylases activity but induces their depression, although it increases NAD+ concentration[48]. Furthermore, NR reduces the high blood pressure and the stiffness of aorta accompanying ageing[27].

CONCLUSION

From this study, it can be concluded that senescence is a systemic process occurs mainly via decreased level of NAD+ with subsequent OS, inflammageing, genomic instability with DNA damage and altered apoptotic process. When these disorders affect the gastric parietal cells, they may result into GIT disturbances (maldigestion, malabsorption, and anorexia) that are frequently associated with ageing. Such GIT manifestations may, consequently, worsen and exaggerate the ageing sequalae via induction of anaemia, and continuous reduction of NAD+. Blockage of most of these manifestations can be achieved by increase NAD+ level through oral supplementation of one of its precursors, especially NR as it has many advantages over the other precursors.

CONFLICT OF INTERESTS

There are no conflicts of interest.

REFERENCES

1. Jones OR, Scheuerlein A, Salguero-Gómez R, Camarda CG, Schaible R, Casper BB, Dahlgren JP, Ehrlén J, García MB, Menges ES, Quintana-Ascencio PF, Caswell H, Baudisch A, Vaupel JW. Diversity of ageing across the tree of life. Nature. 2014; 505:169-73. doi: 10.1038/nature12789
2. Kennedy BK, Berger SL, Brunet A, Campisi J, Cuervo AM, Epel ES, Franceschi C, Lithgow GJ, Morimoto RI, Pessin JE, Rando TA, Richardson A, Schadt EE, Wyss-Coray T, Sierra F. Geroscience: linking ageing to chronic disease. Cell. 2014; 159: 709–13. doi: 10.1016/j.cell.2014.10.039
3. López-Otín C, Blasco MA, Partridge L, Serrano M, Kroemer G. The Hallmarks of Aging. Cell. 2013;153: 1194-217. doi: 10.1016/j.cell.2013.05.039.
4. Tchkonia T, Zhu Y, van Deursen J, Campisi J, Kirkland JL. Cellular senescence and the senescent secretory phenotype: therapeutic opportunities. J Clin Invest. 2013; 123: 966-72. doi: 10.1172/JCI64098.
5. Dumic I, Nordin T, Jecmenica M, Stojkovic Lalosevic M, Milosavljevic T, Milovanovic T. Gastrointestinal Tract Disorders in Older Age. Canadian journal of gastroenterology & hepatology. 2019; Article ID 6757524, 19 pages. doi: 10.1155/2019/6757524.
6. Imai S, Yoshino J. The importance of NAMPT/NAD/SIRT1 in the systemic regulation of metabolism and ageing. Diabetes, obesity & metabolism. 2013;15: 26-33. doi: 10.1111/dom.12171
7. Mehmel M, Jovanović N, Spitz U. Nicotinamide Riboside-The Current State of Research and Therapeutic Uses. Nutrients. 2020; 12:1616. doi: 10.3390/nu12061616.
8. Mericskay M. Nicotinamide adenine dinucleotide homeostasis and signalling in heart disease: Pathophysiological implications and therapeutic potential. Arch. Cardiovasc. Dis. 2016, 109: 207–15. doi: 10.1016/j.acvd.2015.10.004.
9. Benarroch EE. Acquired axonal degeneration and regeneration: Recent insights and clinical correlations. Neurology. 2015; 84: 2076–85. doi: 10.1212/WNL.0000000000001601.

10. Trammell SA, Weidemann BJ, Chadda A, Yorek MS, Holmes A, Coppey LJ, Obrosov A, Kardon RH, Yorek MA, Brenner C. Nicotinamide Riboside Opposes Type 2 Diabetes and Neuropathy in Mice. Sci Rep. 2016; 6:26933. doi: 10.1038/srep26933.

11. Sengupta L. The Laboratory Rat: Relating Its Age with Human's. Int J Prev Med. 2013; 4: 624–30. PMID: 23930179; PMCID: PMC3733029.

12. Marta V. Hamity, Stephanie R. White, Roxanne Y. Walder, Mark S. Schmidt, Charles Brenner, Donna L. Nicotinamide riboside, a form of vitamin B3 and NAD+ precursor, relieves the nociceptive and aversive dimensions of paclitaxel-induced peripheral neuropathy in female rats. Hammond. Pain. 2017; 158: 962–72. doi: 10.1097/j.pain.0000000000000862

13. Feher J. The Stomach. In Quantitative Human Physiology (second edition), Academic Press, 2017, pp 785-95. https://educate.elsevier.com/book/details/9780128008836

14. El-Akabawy G, El-Kholy W. Neuroprotective effect of ginger in the brain of streprozotocin-induced diabetic rats. Ann Anat 2014; 196: 119- 28. doi: 10.1016/j.aanat.2014.01.003.

15. El Agaty SM. Cardioprotective effect of vitamin D2 on isoproterenol-induced myocardial infarction in diabetic rats. Archives of Physiology and Biochemistry. 2019; 125:210-9. doi: 10.1080/13813455.2018.1448423

16. Suvarna K, Layton C, Bancroft J. The hematoxylins and eosin, Immunohistochemical techniques & Transmission electron microscopy. In Bancroft's Theory and Practice of Histological Techniques (Eighth Edition), Elsevier,2019, pp: 126-38, 337-94, 434-75. https://shop.elsevier.com/books/bancrofts-theory-and-practice-of-histological-techniques/suvarna/978-0-7020-6864-5

17. Engevik AC, Kaji I, Goldenring JR. The Physiology of the Gastric Parietal Cell. Physiol Rev. 2020; 100:573-602. doi: 10.1152/physrev.00016

18. Salles N. Basic mechanisms of the aging gastrointestinal tract. Dig Dis. 2007; 25:112-7.

19. Hernandez-Segura A, de Jong TV, Melov S, Guryev V, Campisi J, Demaria M. Unmasking Transcriptional Heterogeneity in Senescent Cells. Curr Biol. 2017; 27:2652-60. e4. doi: 10.1016/j.cub.2017.07.033

20. Imai S, Guarente L. NAD+ and sirtuins in aging and disease. Trends Cell Biol. 2014; 24:464-71. doi: 10.1016/j.tcb.2014.04.002

21. Schultz MB, Sinclair DA. Why NAD (+) Declines during Aging: It's Destroyed. Cell Metab. 2016; 23:965-6. doi: 10.1016/j.cmet.2016.05.022

22. Hernandez-Segura A, Nehme J, Demaria M. Hallmarks of Cellular Senescence. Trends Cell Biol. 2018; 28:436-53. doi: 10.1016/j.tcb.2018.02.001

23. Wiley CD, Velarde MC, Lecot P, Liu S, Sarnoski EA, Freund A, Shirakawa K, Lim HW, Davis SS, Ramanathan A, Gerencser AA, Verdin E, Campisi J. Mitochondrial Dysfunction Induces Senescence with a Distinct Secretory Phenotype. Cell Metab. 2016; 23:303-14. doi: 10.1016/j.cmet.2015.11.011

24. Ragnauth CD, Warren DT, Liu Y, McNair R, Tajsic T, Figg N, Shroff R, Skepper J, Shanahan CM. Prelamin A acts to accelerate smooth muscle cell senescence and is a novel biomarker of human vascular aging. Circulation. 2010; 121:2200-10. doi: 10.1161/CIRCULATIONAHA.109.902056.

25. Ohanna M, Giuliano S, Bonet C, Imbert V, Hofman V, Zangari J, Bille K, Robert C, Bressac-de Paillerets B, Hofman P, Rocchi S, Peyron JF, Lacour JP, Ballotti R, Bertolotto C. Senescent cells develop a PARP-1 and nuclear factor-{kappa}B-associated secretome (PNAS). Genes Dev. 2011; 25:1245-61. doi: 10.1101/gad.625811

26. Lingappan K. NF-κB in Oxidative Stress. Curr Opin Toxicol. 2018; 7:81-6. doi: 10.1016/j.cotox.2017.11.002

27. Martens CR, Denman BA, Mazzo MR, Armstrong ML, Reisdorph N, McQueen MB, Chonchol M, Seals DR. Chronic nicotinamide riboside supplementation is well-tolerated and elevates NAD+ in healthy middle-aged and older adults. Nat Commun. 2018 29; 9:1286. doi: 10.1038/s41467-018-03421-7.

28. Huang T. The Role of NAD+ in Anti-Aging Therapies. American Journal of Biomedical Science & Research. 2019; 6:446-53. DOI: 10.34297/AJBSR.2019.06.001080

29. Tower J. Programmed cell death in aging. Ageing Res Rev. 2015; 23:90-100. doi: 10.1016/j.arr.2015.04.002

30. Muñoz-Espín D, Serrano M. Cellular senescence: from physiology to pathology. Nat Rev Mol Cell Biol. 2014; 15:482-96. doi: 10.1038/nrm3823.

31. Wang AS, Dreesen O. Biomarkers of Cellular Senescence and Skin Aging. Front Genet. 2018 23; 9:247. doi: 10.3389/fgene.2018.00247

32. Sharpless NE, Sherr CJ. Forging a signature of in vivo senescence. Nat Rev Cancer. 2015; 15:397-408. doi: 10.1038/nrc3960

33. Majumdar AP: Regulation of gastrointestinal mucosal growth during aging. J Physiol Pharmacol. 2003; 54:143–54. PMID: 15075456. https://pubmed.ncbi.nlm.nih.gov/15075456/

34. Irie-Maezono R, Tsuyama S. Immunohistochemical Analysis of the Acid Secretion Potency in Gastric Parietal Cells. CellBio. 2013;2: Article ID:40429, 179-185. DOI: 10.4236/cellbio.2013.24020

35. Schubert ML. Gastric acid secretion. Curr Opin. Gastroenterol. 2016; 32:452-60. doi: 10.1097/MOG.0000000000000308

36. Magris R, De Re V, Maiero S, Fornasarig M, Guarnieri G, Caggiari L, Mazzon C, Zanette G, Steffan A, Canzonieri V, Cannizzaro R. Low Pepsinogen I/II Ratio and High Gastrin-17 Levels Typify Chronic Atrophic Autoimmune Gastritis Patients with Gastric Neuroendocrine Tumors. Clin Transl Gastroenterol. 2020;11: e00238. doi: 10.14309/ctg.0000000000000238

37. Keller J, Layer P. The Pathophysiology of Malabsorption. Viszeralmedizin. 2014; 30:150-4. doi: 10.1159/000364794.

38. Washabau RJ. Integration of Gastrointestinal Function. In: Canine and Feline Gastroenterology. Elsevier Inc, 2013: pp 1-31. https://doi.org/10.1016/B978-1-4160-3661-6.00001-8

39. Azuma T, Suto H, Ito Y, Ohtani M, Dojo M, Kuriyama M, Kato T. Gastric leptin and Helicobacter pylori infection. Gut. 2001; 49:324-9. doi: 10.1136/gut.49.3.324.

40. Williams J, Mobarhan S. A critical interaction: leptin and ghrelin. Nutr Rev. 2003; 61:391–3. doi: 10.1301/nr.2003.nov.391-393

41. Waldum HL, Kleveland PM, Sørdal ØF. Helicobacter pylori and gastric acid: an intimate and reciprocal relationship. Therap Adv Gastroenterol. 2016; 9:836-44. doi: 10.1177/1756283X16663395.

42. Johnson S, Imai SI. NAD + biosynthesis, aging, and disease. F1000Res. 2018; 7:132. doi: 10.12688/f1000research.12120.1.

43. Camacho-Pereira J, Tarragó MG, Chini CCS, Nin V, Escande C, Warner GM, Puranik AS, Schoon RA, Reid JM, Galina A, Chini EN. CD38 Dictates Age-Related NAD Decline and Mitochondrial Dysfunction through an SIRT3-Dependent Mechanism. Cell Metab. 2016; 23:1127-39. doi: 10.1016/j.cmet.2016.05.006

44. Tirumurugaan KG, Kang BN, Panettieri RA, Foster DN, Walseth TF, Kannan MS. Regulation of the cd38 promoter in human airway smooth muscle cells by TNF-alpha and dexamethasone. Respir Res. 2008; 9:26. doi: 10.1186/1465-9921-9-26.

45. Aman Y, Qiu Y, Tao J, Fang EF. Therapeutic potential of boosting NAD+ in aging and age-related diseases. Translational Medicine of Aging. 2018;2: 30-7. DOI: 10.1016/j.tma.2018.08.003

46. Trammell SA, Schmidt MS, Weidemann BJ, Redpath P, Jaksch F, Dellinger RW, Li Z, Abel ED, Migaud ME, Brenner C. Nicotinamide riboside is uniquely and orally bioavailable in mice and humans. Nat Commun. 2016 10; 7:12948. doi: 10.1038/ncomms12948.

47. Bogan KL, Brenner C. Nicotinic acid, nicotinamide, and nicotinamide riboside: a molecular evaluation of NAD+ precursor vitamins in human nutrition. Annu Rev Nutr. 2008; 28:115-30. doi: 10.1146/annurev.nutr.28.061807.155443

48. Guan X, Lin P, Knoll E, Chakrabarti R. Mechanism of inhibition of the human sirtuin enzyme SIRT3 by nicotinamide: computational and experimental studies. PLoS One. 2014 15;9: e107729. doi: 10.1371/journal.pone.0107729.

الملخص العربى

تأثير الشيخوخة على الخلايا الجدارية المَعِدية في ذكور الجرذان البيضاء ودور نيكوتيناميد ريبوسيد) أحد سلائف نيكوتيناميد الأدينين ثنائي النوكليوتيد): دراسة هستولوجية

مروة محمد يسرى،عبير إبراهيم عمر،ايمان عباس فرج

قسم الهستولوجي، كلية الطب، جامعة القاهرة، مصر

الخلفية: تعتبر الشيخوخة تعاقب طبيعي في الوقت ونضج الخلية، مع تغييرات خلوية تركيبية وظيفية تدريجية. وهو عامل مؤهب رئيسي للعديد من الأمراض غير المُعْدِية مثل أمراض القلب والأوعية الدموية وأمراض التمثيل الغذائي والأمراض التنكسية العصبية والأمراض السرطانية ويلحق ذلك ارتفاع معدلات الإصابة والوفيات. عادة ما ترتبط أعراض الجهاز الهضمي بالشيخوخة بدءًا من التهاب الفم إلى سوء الهضم وسوء الإمتصاص. ينخفض نيكوتيناميد الأدينين ثنائي النوكليوتيد، الإنزيم المشترك في تفاعلات الفسفرة المؤكسدة وتفاعلات الأكسدة والاختزال في التمثيل الغذائي وإنتاج الطاقة، في العديد من الحالات المرضية المرتبطة بالشيخوخة ويظهر استعاده مستواه تحسنًا ملحوظًا في هذه الحالات.

هدف العمل: هدفت هذه الدراسة إلى تقييم عواقب الشيخوخة على الخلايا الجدارية المَعِدية في ذكور الجرذان البيضاء، والدور المحتمل لنيكوتيناميد الأدينين ثنائي النوكليوتيد، والدور الوقائي المحتمل للنيكوتيناميد ريبوسيد (أحد سلائف نيكوتيناميد الأدينين ثنائي النوكليوتيد).

المواد وطرق البحث: تم تقسيم ١٨ من ذكورالجرذان البيضاء بالتساوي إلى المجموعة الضابطة [حوالي ٣ أشهر، المجموعة الأولى]، المجموعة المسنة [حوالي ٢٤ شهرًا، المجموعة الثانية] والمجموعة المسنة / نيكوتيناميد ريبوسيد [حوالي ٢٤ شهرًا، المجموعة الثالثة] التي تلقت ٢٠٠ مجم / كجم من نيكوتيناميد ريبوسيد جرعة واحدة يوميًا عن طريق الفم لمدة ٣ أسابيع. قبل التضحية مباشرة، تم تقييم المستويات المَصْلِيّة للنيكوتيناميد ريبوسيد وجاسترين وبيبسينوجين-١ لجميع الحيوانات. أجريت بعد ذلك الدراسات الكيميائية الحيوية والنسيجية والكيميائية المناعية للـهيدروجين بوتاسيوم أَتَباز وبي سي إل -٢ والدراسات المترية الشكلية.

النتائج: تحسنت سمات الشيخوخة التي ظهرت في الخلايا الجدارية للجرذان المسنة بشكل ملحوظ مع تناول النيكوتيناميد ريبوسيد (أحد سلائف نيكوتيناميد الأدينين ثنائي النوكليوتيد) لمدة٣ أسابيع عن طريق الفم.

الاستنتاج: الشيخوخة هي عملية شاملة يقل فيها نيكوتيناميد الأدينين ثنائي النوكليوتيد والإجهاد التأكسدي الناتج، والشيخوخة الالتهابية، وتلف الحمض النووي وتغير موت الخلايا المبرمج. يؤدي شيخوخة الخلايا الجدارية إلى اضطرابات الجهاز الهضمي التي قد تؤدي إلى تفاقم عواقب الشيخوخة من خلال تحفيز فقر الدم، والتقليل المستمر لنيكوتيناميد الأدينين ثنائي النوكليوتيد. يمكن منع أغلب هذه الاعراض بتناول مكملات سلائف نيكوتيناميد الأدينين ثنائي النوكليوتيد عن طريق الفم، خاصة النيكوتيناميد ريبوسيد لأنه يتمتع بالعديد من المزايا عن الآخرين.